

The subthermal excitation of the CI lines in the molecular gas reservoirs of galaxies: its significance and potential utility

P. Papadopoulos^{1,2,3*}, L. Dunne,² & S. Maddox,²

¹ Department of Physics, Section of Astrophysics, Astronomy and Mechanics, Aristotle University of Thessaloniki, Thessaloniki, GR-54124, Greece

² School of Physics and Astronomy, Cardiff University, Queens Buildings, The Parade, Cardiff, CF24 3AA, UK

³ Research Center for Astronomy, Academy of Athens, Soranou Efessiou 4, GR-11527, Athens, Greece

Accepted 2021 October 27. Received 2021 October 22; in original form 2021 June 24

ABSTRACT

We examine a sample of 106 galaxies for which the total luminosities of the two fine structure lines $^3P_1 \rightarrow ^3P_0$, and $^3P_2 \rightarrow ^3P_1$ of neutral atomic carbon (C) are available, and find their average excitation conditions to be strongly subthermal. This is deduced from the CI(2-1)/(1-0) ratios ($R_{21/10}^{(ci)}$) modeled by the exact solutions of the corresponding 3-level system, without any special assumptions about the kinematic state of the concomitant H₂ gas (and thus the corresponding line formation mechanism). This non-LTE excitation of the CI lines can induce the curious clustering of (CI,LTE)-derived gas temperatures near ~25 K reported recently by Valentino et al. (2020), which is uncorellated to the actual gas temperatures. The non-LTE CI line excitation in the ISM of galaxies deprives us from a simple method for estimating molecular gas temperatures, and adds uncertainty in CI-based molecular gas mass estimates especially when the J=2–1 line is used. However the $R_{21/10}^{(ci)} = F(n, T_k)$ ratio is now more valuable for joint CO/CI SLED and dust SED models of galaxies, and independent of the assumptions used in the CO radiative transfer models (e.g. the LVG approximation). Finally we speculate that the combination of low ratios $R_{21/10}^{(ci)} \lesssim 1$ and high T_{dust} values found in some extreme starbursts indicates massive low-density molecular wind and/or circumgalactic gas reservoirs. If verified by imaging observations this can be a useful indicator of the presence of such reservoirs in galaxies.

Key words: galaxies: ISM – ISM: molecules – (ISM:) cosmic rays – ISM: atoms – galaxies: starburst

1 INTRODUCTION

The standard Photon-Dominated Region (PDR) view has the CI line emission emanating only from a C-rich transition layer between the outer CII-rich and the inner CO-rich regions of FUV-irradiated molecular clouds, because of a sharp recombination of ionized Carbon to neutral carbon and then to CO. This was observed recently in small regions near the Be star ρ Ophiuchi using ALMA but in the same image an extended CI-rich molecular gas component is hard to contain in the standard PDR picture (Yamagishi et al. 2021). The first observations challenging a PDR-only origin of the CI line emission in the ISM were obtained by Keene et al (1985, 1986) and Plume et al. (1994), showing the CI $^3P_1 \rightarrow ^3P_0$ (henceforth CI 1-0) line emission persisting well past PDR fronts, deep inside CO-rich molecular clouds and even in a FUV-shielded dark cloud. Since then a widespread (CO, ¹³CO)-C concomitance has been established for the Orion A, B molecular clouds (Ikeda et al. 2002), the Galactic

Center (Ojha et al 2001; Tanaka et al. 2011), cold dark and FUV-shielded clouds in the Galaxy (Oka et al. 2001), and a similar such cloud in M 31 (Israel, Tilanus, & Baas 1998). CI 1-0 line emission is detected in very FUV-shielded regions deep inside classical “dark” clouds such as TMC-1 (Tatematsu et al. 1999) and Bok globules like Barnard 68. In the latter the CI 1-0 line is brighter than what PDR models that fit the CO, ¹³CO lines predict, and Cosmic Rays (CRs) seem necessary to explain the molecular gas thermal state (Pineda & Bench 2007).

Nevertheless, theoretical prejudices “conspired” with the demanding nature of the CI 1-0 line observations at 492 GHz and the lack of multi-beam receivers capable for rapid CI line mapping in the few places on Earth where such observations are possible (Mauna Kea/Hawaii, the Atacama desert Plateau in Chile, and Antarctica) to keep intact the notion of CI lines emanating only from a narrow CII/CI/CO transition layer in the outer regions of molecular clouds. A comprehensive theoretical and observational case for a C/CO concomitance in molecular clouds, with CI lines an alternative molecular gas mass tracer over large scales, was made (Papadopoulos,

* E-mail: padelis@auth.gr

Thi, & Viti 2004) and boils down to: a) cosmic rays controlling the C/CO abundance throughout the FUV-shielded volumes of molecular clouds, b) a strong turbulent mixing of any initial FUV-induced CII/CI/CO species stratification, and c) a non-equilibrium chemistry operating within finite-age molecular clouds ($T_{\text{age}} \lesssim 10^7$ yrs: the chemical and dynamical "recycle" time for the $\text{H}_2 \rightarrow \text{HI}$ phase transition). In vigorously star-forming galaxies all three factors will further enhance the [C/CO] abundance throughout the molecular clouds. Clumpy molecular cloud structures (e.g. Stutzki et al. 1998) can maintain some of the observed C and CO concomitance deeper than expected from uniform FUV-irradiated cloud "surfaces" without fundamentally altering the static PDR carbon-species stratification picture (Spaans & van Dishoeck 1997), but are hard-pressed to explain the tight CI-(^{13}CO , ^{12}CO) *brightness correlation* and the similar CO, C line profiles observed over a wide range of ISM conditions (Papadopoulos et al. 2004).

Recent theoretical work on the role of CRs (Bisbas, Papadopoulos, & Viti 2015; Bisbas et al. 2017), as well as turbulent cloud simulations incorporating the chemical network controlling the C/CO abundance (Offner et al. 2014; Glover et al. 2015; Glover & Clark 2016; Clark et al. 2019) have largely borne this picture out. However it was the large accumulation of CI line data in the extragalactic Universe, that marked a true advance of our views about the regions and conditions where these two lines emanate in molecular gas.

The Herschel Space Observatory (HSO) yielded large CI line datasets for Luminous Infrared Galaxies (LIRGs) in the local Universe (e.g. Pereira-Santaella et al. 2013; Schirm et al. 2014; Kamenetzky et al. 2014; Papadopoulos et al. 2014; Israel, Rosenberg & van der Werf 2015; Lu et al. 2017; Crocker et al. 2019), while earlier efforts took advantage of large redshifts bringing the CI lines to more favorable atmospheric windows, to detect starburst and AGN in the distant Universe (Weiss et al. 2003, 2007; Walter et al. 2011; Schumacher et al. 2012; Canāmeras et al. 2018; Nesvadba et al. 2019). The onset of ALMA operations at the dry high plateau of the Atacama desert generated spectacular amounts of CI line data both locally (Cicone et al. 2018; Miyamoto et al. 2018; Jiao et al. 2017, 2019; Salak et al. 2019; Michiyama et al. 2020; Saito et al. 2020; Izumi et al. 2020; Miyamoto et al. 2021; Dunne et al. 2021), and in the distant Universe (e.g. Alaghband-Zadeh et al. 2013; Bothwell et al. 2017; Popping et al. 2017; Emonts et al. 2018; Andreani et al. 2018; Lu et al. 2018; Banerji et al. 2018; Lelli et al. 2018; Valentino et al. 2018, 2020; Man et al. 2019; Harrington et al. 2021; Boogaard et al. 2020).

The aforementioned observations paint a consistent picture of concomitant C and CO, with CI 1-0 a viable alternative H_2 mass tracer at the scales examined. Nevertheless there are cases with the CI (1-0) line remaining undetected in CO-detected regions (Michiyama et al. 2020; Miyamoto et al. 2021), and the other way around (Dunne et al. 2021). More observational work is necessary for these outliers to probe the possibility of very different *global* ISM conditions, and address possible sensitivity issues in detecting the fainter CI 1-0 emission expected in CO-rich but cold and denser gas. In the most recent CI 1-0, 2-1 line dataset analysed by Valentino et al. 2020 for Main Sequence galaxies at $z \sim 1$ the (CI, LTE)-derived gas temperatures cluster around $\langle T_{\text{k}}(\text{CI, LTE}) \rangle \sim 26$ K, are $\lesssim T_{\text{dust}}$, and have a dispersion of $\sigma(T) \sim 8$ K. If these are actual average T_{kin} values for the molecular gas, they are hard to reconcile with typical (CO SLED)-derived T_{kin} values for SF galaxies in the local Universe where $T_{\text{kin}} \sim (30-100)$ K (e.g. Wall et al. 1993; Aalto et al. 1995; Papadopoulos et al. 2010a; Kamenetzky et al. 2014).

In this work the largest extragalactic CI 2-1, 1-0 line dataset

to date is used to examine the average CI line excitation conditions by using: a) the exact analytical solutions of the CI 3-level system, and b) the dust temperatures obtained from dust emission Spectral Energy Distributions (SEDs) available for our sample. We find the CI lines to be globally subthermally excited in the ISM of galaxies, discuss its impact on molecular gas temperature and mass estimates, and the utility of a non-LTE CI 2-1/1-0 ratio $R_{21/10}^{(\text{ci})} = F(n, T_{\text{kin}})$ in joint models with global CO SLEDs, and dust SEDs of galaxies. Finally we highlight the possibility of using $R_{21/10}^{(\text{ci})}$ versus the T_{dust} extracted from global dust emission SEDs as an indicator of massive molecular gas winds and/or circumgalactic gas reservoirs around starburst galaxies.

2 THE CI LINE AND DUST CONTINUUM DATA

We canvassed the literature for all available CI 2-1, 1-0 line data for galaxies that also have submm/FIR dust continuum data adequate to provide an estimate of the luminosity-weighted T_{dust} from the fitting of a modified black-body (MBB). This yields 106 sources, ranging from nearby quiescently star forming galaxies (e.g. NGC891) and local (U)LIRGs to high redshift lensed submillimeter galaxies (SMG) and QSO with a range of $L_{\text{IR}} \sim (10^9 - 5 \times 10^{13}) L_{\odot}$ (values corrected for lensing). Using conversion between SFR and L_{IR} of 1.5×10^{-10} , Kennicutt & Evans 2012; Hao et al. 2011; Murphy et al. 2011), this corresponds to $\text{SFR} \sim 0.15-8000 M_{\odot} \text{ yr}^{-1}$, i.e. from the very quiescent to the extreme starburst SF activity level. The sample (presented in full in Dunne et al. *in prep*) is drawn from the following literature sources: (Alaghband-Zadeh et al. 2013; Aniano et al. 2020; Chang et al. 2020; Chu et al. 2017; Clark et al. 2018; Crocker et al. 2019; Jiao et al. 2017, 2019, 2021; Garcia-Gonzalez et al. 2016; Harrington et al. 2021, Israel et al. 2015; Kamenetzky et al. 2014; Lapham & Young 2019; Liu et al. 2015, 2021; Lu et al. 2017, Nesvadba et al. 2019; Papadopoulos et al. 2010a; Pereira-Santaella et al. 2013; Rosenberg et al. 2015; Schumacher et al. 2012; Stacey et al. 2018; Valentino et al. 2018, 2020; Walter et al. 2011).

In this work we use a simple but effective argument based on the thermal decoupling of gas and dust to set lower limits on the average T_{k} of the molecular gas reservoirs in the sources of our sample using average T_{d} values (see Section 2.3.1). In this manner we avoid the well-known difficulties of determining the average T_{k} of molecular gas which requires well-sampled CO SLEDs, including optically thin isotopologues, and tracers of high density gas in order to break the T_{k} -n degeneracies inherent in LVG modelling (e.g. Papadopoulos et al. 2014). Needless to say that such difficulties are massively compounded by the size of our sample as well as the non-uniformity of the molecular, and atomic SLEDs available for each object. Now in order to determine the average T_{d} values the MBB models use data at $\lambda_{\text{rest}} > 60 \mu\text{m}$, while shorter wavelength data, if available, set an upper limit to the warm dust mass (at $\lambda_{\text{rest}} < 60 \mu\text{m}$ the dust SED diverges from a MBB due to transiently heated small grains, PAH and/or hot AGN-powered components). We use $\beta = 1.8$ for the fits, where the literature source provided a fit using a similar method we use their results, otherwise we re-fitted the published photometry ourselves¹.

We recognize that one-component dust continuum fits are overly simple, and for global (i.e. spatially unresolved) SEDs tend to be dominated by the warmer dust component(s). They are however adequate for our purpose of using the deduced luminosity-weighted

¹ Other sources of FIR data: Chu et al. (2017), Clark et al. (2018).

T_{dust} values to normalize the $T_{\text{kin}}(\text{CI, LTE})$ values extracted from a similarly one-component modeled $R_{21/10}^{(\text{ci})}$ ratio. This is because even for modestly FUV-irradiated/CR-innuded molecular clouds in SF galaxies, gas with $n \lesssim 10^4 \text{ cm}^{-3}$ will be CI-rich and warm (Papadopoulos, Thi, & Viti 2004; Papadopoulos et al. 2011) while containing also the bulk of the gas (and thus dust) mass per molecular cloud². The collective emission of such clouds will thus dominate the global CO, CI SLEDs and dust emission SEDs in galaxies (a possible large scale deviation from this simple picture is discussed in Section 3.1).

2.1 The cases of high dust optical depth.

Some compact starbursts and/or deeply dust-enshrouded AGN in our sample may have dust SEDs that are optically thick well into the FIR/sub-mm (e.g. Arp220, GN20: Papadopoulos 2010b; Scoville et al. 2015; Cortzen et al. 2020). This has two main effects:

(i) The isothermal luminosity-weighted dust temperature, fitted under the assumption of optically thin emission under-estimates the true T_{dust} in an optically thick dust SED as the submm "excess" due to high dust optical depths will be attributed to colder dust. Thus the true $T_{\text{d}}(\tau)$ will be higher than from that obtained under an optically thin MBB.

(ii) The observed ratio of C I 2-1/1-0 is suppressed by the differing dust optical depths between the two frequencies and must be corrected in order to recover the intrinsic ratio, and hence the intrinsic $T_{\text{kin}}(\text{CI, LTE})$.

This correction is discussed in Papadopoulos (2010b) and can be expressed as:

$$R_{21/10}^{(\text{ci})}(\text{int}) = R_{21/10}^{(\text{ci})}(\text{obs}) \times \exp[\tau_{\text{d}}(\nu_{21}) - \tau_{\text{d}}(\nu_{10})] \quad (1)$$

where $\tau_{\text{d}}(\nu)$ is the dust optical depth at the frequencies ν_{21} (809 GHz) and ν_{10} (492 GHz) of the C I lines, and

$$R_{21/10}^{(\text{ci})} = \frac{\int_{\Delta V} S_{\text{CI}}(2-1)dV}{\int_{\Delta V} S_{\text{CI}}(1-0)dV}, \quad (2)$$

is the C I (2-1)/(1-0) line ratio ($\int_{\Delta V} S_{\text{CI}}dV$ in Jy km s^{-1} : the velocity-integrated line flux density), with (int) and (obs) designating the intrinsic (i.e. τ_{d} -corrected) and observed values respectively. The corrections obtained for the optically thick sources are ~ 1.2 – 2.8 (the highest value in Arp220), and shift the CI line ratios of a few optically thick sources (GN20, IRAS F 10214, AMS 12) to higher corresponding densities and almost into the LTE excitation domain (see discussion in 2.4)

The dust SED fits are *highly degenerate* between solutions with a higher dust optical depth, and those with a larger range of temperatures contributing to the SED. We therefore only use the optically thick parameters for 6 local (U)LIRGs where other evidence supports very compact bright regions producing the IR emission (e.g. interferometric imaging showing very high mm surface brightness, evidence for X-ray absorbed AGN, severe deficit of C[II] relative to L_{IR} , or high brightnesses of emission lines (e.g.

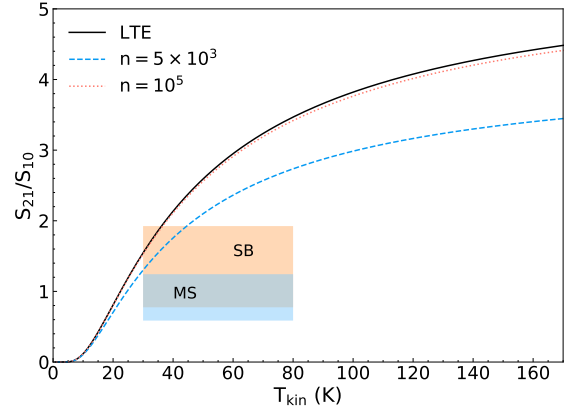


Figure 1. The $R_{21/10}^{(\text{ci})} = S_{21}/S_{10} = F(T_{\text{kin}}, n)$ line ratio (S_{21}, S_{10} in Jy km s^{-1}) versus T_{k} , computed using the analytical non-LTE expressions for a 3-level system, in the optically thin regime. We show 3 cases: full LTE (black line), $n = 10^5 \text{ cm}^{-3}$ (red dotted line), and $n = 5 \times 10^3 \text{ cm}^{-3}$ (blue dashed line). The critical density of the C I (2-1) line $n_{21, \text{crit}} \sim 10^3 \text{ cm}^{-3}$. The shaded regions: (vertical) the 1σ range of the $R_{21/10}^{(\text{ci})}$ values in our sample (salmon: starbursts, blue: main-sequence (MS) galaxies), (horizontal) the typical T_{k} range deduced from CO SLED modelling in literature studies.

HCN-*vib*) that are only excited in the presence of extreme IR radiation fields (González-Alfonso & Sakamoto 2019, Boettcher et al. 2020; Falstad et al. 2021). Not all these sources have extreme L_{IR} ; NGC 4418 and Zw 049.057 are examples of moderate $L_{\text{IR}} \sim 2 \times 10^{11} L_{\odot}$ sources with very dense and compact dust regions ($N_{\text{H}} \gtrsim 10^{25} \text{ cm}^{-3}$).³ Additionally, we use optically thick corrections to C I line ratios for 16 high- z SMG/QSO which were fitted with $T_{\text{d}}(\tau) > 50 \text{ K}$, and had enough data points to exclude a simple isothermal optically thin SED. In total we apply such corrections to 22 sources, and show the results with and without the optical depth corrections (see 2.4).

2.2 The non-LTE excitation of the C I 1-0, 2-1 lines

For the C I lines it is: $T_1 = E_1/k_{\text{B}} = 23.6 \text{ K}$ and $E_2/k_{\text{B}} = 62.4 \text{ K}$, while the T_{kin} values from SLED fits of extragalactic CO lines are typically $T_{\text{kin}}(\text{CO SLED}) \sim (30\text{--}100) \text{ K}$ (i.e. nearly "bracketed" by E_1/k_{B} and E_2/k_{B}). A purely-LTE C I line excitation, with $T_{\text{kin}}(\text{CI, LTE}) \sim T_{\text{kin}}(\text{CO SLED})$, should then yield a $R_{21/10}^{(\text{ci})}$ ratio that is strongly T_{kin} -variable throughout this T_{k} range. In Figure 1 we plot the analytical expression of $R_{21/10}^{(\text{ci})} = F(n, T_{\text{kin}})$ (using formulas taken from Papadopoulos, Thi & Viti 2004, Appendix) where it can be seen that for $T_{\text{kin}}(\text{LTE, CI}) \sim 30\text{--}100 \text{ K}$ the $R_{21/10}^{(\text{ci})}(\text{LTE})$ ratio indeed varies significantly ($\sim 1\text{--}3.8$), but also that most of the *observed* $R_{21/10}^{(\text{ci})}$ values, lie well below the corresponding LTE values.

An educational aspect of Figure 1 is the demonstration that $R_{21/10}^{(\text{ci})}$ remains below its purely-LTE values even for densities as high as $n = 5 \times 10^3 \text{ cm}^{-3}$ ($\sim 5 \times$ the critical density of C I 2-1). This means that spectral line thermalization is a very gradual function of n/n_{crit} , and that the often encountered assertion that a spectral line reaches LTE conditions when gas densities reach $n \sim n_{\text{crit}}$ is incorrect.

² Even for the highly turbulent ISM of merger/starburst systems observations show at most $\sim 25\%$ of molecular gas mass to reside at densities $> 10^4 \text{ cm}^{-3}$ (Gao & Solomon 2004).

³ The observed $T_{\text{kin}}(\text{CI, LTE})$ of these sources are very low 13–18 K, further supporting the necessity of optical depth corrections.

Finally from Figure 1 we can see also that the gas temperatures corresponding to the measured $R_{21/10}^{(ci)}$ line ratios under the LTE assumption, namely:

$$T_{\text{kin}}(\text{CI, LTE}) = \frac{38.8 \text{ K}}{\ln\left(5.63/R_{21/10}^{(ci)}\right)} \quad (3)$$

(for $E_{21}/k_B=38.8 \text{ K}$, $A_{21}=2.68 \times 10^{-7} \text{ s}^{-1}$, $A_{10}=7.93 \times 10^{-8} \text{ s}^{-1}$, Zmuidzinas et al. 1988) will all gather in a relatively narrow range of $T_{\text{kin}}(\text{CI, LTE}) \sim (20\text{--}30) \text{ K}$ (if one "projects" the lower and the upper line marking the $1\text{-}\sigma$ width onto the black LTE curve, and then "reads" off the corresponding temperatures of the thus projected points). This is another manifestation of non-LTE conditions which we discuss further in Section 3.

We must mention that piecemeal observational evidence for global subthermal excitation of CI lines has been available for some time. The earliest examples of $T_{\text{kin}}(\text{CI, LTE})$ (T_{kin} deduced from the CI lines under the LTE assumption, Equation 3) being lower than $T_{\text{kin}}(\text{CO SLED})$ and T_{dust} , were reported by Kamenetzky et al. (2014) and Schumacher et al. (2012). The former found $\langle T_{\text{kin}}(\text{CI, LTE}) \rangle = (29 \pm 6) \text{ K} \lesssim T_{\text{dust}}$, and uncorrelated to the $T_{\text{kin}}(\text{CO SLED})$ values, while the later deduced $T_{\text{kin}}(\text{CI, LTE}) < (T_{\text{dust}}, T_{\text{kin}}(\text{CO SLED}))$ for a distant quasar. Both interpreted these temperature differences as due to different ISM regions sampled by the CO, CI lines and the dust continuum rather than large scale sub-thermal CI line excitation. Only in the most recent study of Lensed Planck-selected (LP) galaxies by Harrington et al. (2021) the possibility of global subthermal CI line excitation was recognized, although their argument about enhanced gas kinetic temperatures with respect to carbon excitation temperatures is unclear.

2.3 The CI line excitation, the detailed picture

In Figures 2, 3 we show the $T_{\text{kin}}(\text{CI, LTE})$ versus T_{dust} , and $T_{\text{kin}} = \alpha T_{\text{dust}}$ ($\alpha \geq 1$), the gas temperature expected for a given T_{dust} and an ISM with primary gas heating mechanisms the photoelectric effect induced on dust by FUV radiation (from O, B stars), cosmic rays (CRs), and/or shocks (see section 2.3.1 for details and the adopted values for parameter α).

These figures make it obvious that the *CI lines are globally subthermally excited in the ISM of galaxies* since $T_{\text{kin}}(\text{CI, LTE})$ is lower than T_{dust} , and lower still than the expected $T_{\text{kin}} = \alpha T_{\text{dust}}$ in all but a few objects in our sample. For starbursts, where higher α values are expected for their intensely CR-irradiated ISM, the $T_{\text{kin}}(\text{CI, LTE}) < T_{\text{kin}} = (\alpha T_{\text{dust}})$ inequality is even more pronounced, indicating very subthermal CI line excitation in their H_2 gas reservoirs (see also discussion in 3.1).

In retrospect the global subthermal CI line excitation in the ISM of galaxies should not be so surprising since most of the mass in molecular clouds, even very turbulent ones, lies at densities $n < 10^4 \text{ cm}^{-3}$, where the CI(2-1) line remains subthermally excited (see section 2.2). Furthermore, for CR-irradiated clouds, the $[\text{CI}/\text{H}_2]$ abundance can be $\sim (5\text{--}10) \times$ higher in lower-density ($n \lesssim (\text{few}) \times 10^3 \text{ cm}^{-3}$) than higher density ($\geq 10^4 \text{ cm}^{-3}$) gas (Papadopoulos et al. 2011), making the lower density (and typically the

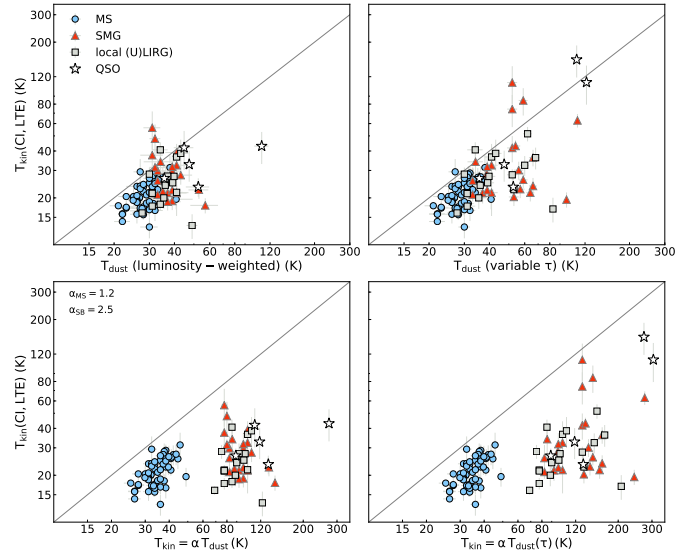


Figure 2. **Top left:** $T_{\text{kin}}(\text{CI, LTE})$ versus T_{d} . The *minimum* values of $T_{\text{kin}}(\text{CI, LTE}) = T_{\text{d}}$ ($\alpha=1$) expected for concomitant gas and dust mass reservoirs (see Section 2.3.1) are marked by a solid line. The luminosity-weighted dust temperature was obtained from the dust SEDs of our sample using optically thin MBB fits at $\lambda_r > 60 \mu\text{m}$ with $\beta=1.8$. **Top right:** As top left but correcting for sources which are plausibly optically thick in the FIR-submm part of the dust SED, by using dust SED fits that include a characteristic optical depth as a free parameter, and correcting $R_{21/10}^{(ci)}$ (and hence $T_{\text{kin}}(\text{CI, LTE})$) accordingly (Section 2.1) **Lower left:** $T_{\text{kin}}(\text{CI, LTE})$ versus the T_{k} expected for the computed T_{d} , with a solid line marking $T_{\text{kin}}(\text{CI, LTE}) = T_{\text{k}}$ (which would be satisfied for the LTE regime). We adopted $\alpha_{\text{MS}}=1.2$ for typical SF galaxies on the ‘Main Sequence’ (MS), and $\alpha_{\text{SB}}=2.5$ for ‘extreme starbursts’ (ULIRGs/SMG/QSO) (see Section 2.3.1). **Lower right:** As in lower left, left but correcting for optically thick dust SEDs.

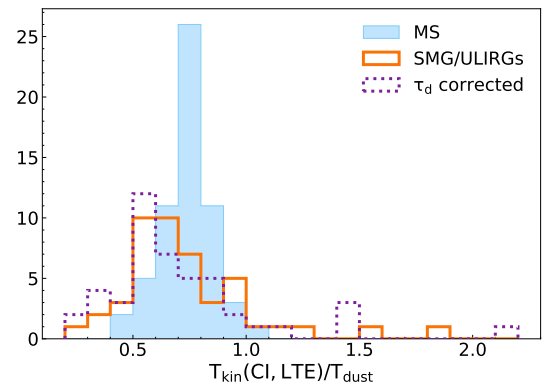


Figure 3. The distribution of the $T_{\text{kin}}(\text{CI, LTE}) / T_{\text{d}}$ ratio, colour coded by the SF mode (normal=blue, extreme=orange). The purple dotted line represents the distribution for the extreme SF sources (SMG/(U)LIRGs) where corrections have been made to account for high optical depth in the dust SED of 22 sources (see Section 2.1). There is no significant difference in the distribution of $T_{\text{kin}}(\text{CI, LTE}) / T_{\text{d}}$ whether optically thick fits are considered or not. Overall the SMG/ULIRG sources have a wider spread of ratios, but both galaxy classes are significantly below the minimum value $T_{\text{k}} = T_{\text{d}}$, with a mean $\langle T_{\text{kin}}(\text{CI, LTE}) / T_{\text{d}} \rangle = 0.73 \pm 0.17$.

most massive) H₂ gas phase the most C-rich one in Giant Molecular Clouds (GMCs)⁴.

2.3.1 A note on the $T_{\text{kin}} \gtrsim T_{\text{dust}}$ gas-dust thermal decoupling, and the choice of α

A key assumption used in this work is that $T_{\text{kin}} = \alpha T_{\text{dust}}$, with $\alpha \geq 1$ holds for most of the molecular gas mass in galaxies. This is both theoretically expected and actually observed. Early PDR models yielded this inequality in FUV-irradiated clouds (e.g. Hollenbach & Tielens 1999, Figure 16) with $T_{\text{kin}} \sim T_{\text{dust}}$ (i.e. gas-dust thermal coupling) occurring only at $A_V \gtrsim 6-10$ in small dense regions deep inside H₂ clouds, where both gas and dust are cold. Deeper in such regions T_{kin} can become lower than T_{dust} by a few Kelvin (e.g. Papadopoulos et al. 2011; see also Hollenbach et al. 1991 for earlier seminal work) which, for the purpose of extragalactic line and dust emission models, are essentially equal. Furthermore such $T_{\text{dust}} \gtrsim T_{\text{kin}}$ regions will be inconspicuous in the emergent (H₂ cloud)-scale (and thus galaxy-scale) line and dust continuum luminosities, even in SF-quietest spirals like the Milky Way with much of their ISM already cold (~ 20 K). This is simply because such regions are typically colder still ($\sim 8-10$ K), and contain only few% of an H₂ cloud's mass⁵.

Beyond the FUV-induced photoelectric heating maintaining $T_{\text{kin}} \gtrsim T_{\text{dust}}$ throughout most of H₂ cloud volumes, it is the *volumetric* cosmic ray (CR)-heating of the gas (but not the dust) that decisively sets a $T_{\text{kin}} > T_{\text{dust}}$ inequality throughout H₂ clouds (Papadopoulos et al. 2011). Even for modest CR energy density enhancements, corresponding to $\sim 10\times$ higher SFR densities than in the Milky Way, CR heating can maintain $T_{\text{kin}} > T_{\text{dust}}$ for densities even up to $\sim 10^5 \text{ cm}^{-3}$ (and thus for the bulk of an H₂ cloud's mass).

Finally we note that turbulence, like CRs (and unlike FUV radiation), will *volumetrically* heat the gas but not the dust. Thus it can only strengthen the original FUV/CR-induced $T_{\text{kin}} > T_{\text{dust}}$ inequality throughout molecular clouds. Observational evidence for this, using multi-species, multi-J SLEDs and submm dust continuum maps, is available for the turbulent molecular gas in the Galactic Center (Papadopoulos et al. 2014 and references therein). In the highly turbulent ISM of extreme starbursts, typically driven by mergers, the shock-dominated turbulent gas heating can be significant and perhaps even dominant.

For ordinary SF systems up to the so-called Main Sequence (MS) galaxies we adopt $\alpha = 1.2$, the minimum value expected for gas and dust temperatures deep inside FUV/CR-irradiated clouds (see Figure 2, Papadopoulos et al. 2011), which can actually be higher (~ 2) for the CR energy densities expected for the upper SFR range of MS galaxies. For starbursts ($\text{SFR} > 100 M_{\odot} \text{ yr}^{-1}$) we adopt $\alpha = 2.5$, a value deduced recently for such galaxies from joint multi-J CO/CI SLED and dust SED fits by Harrington et al. (2021), and readily supported by detailed thermo-chemical calculations for the strongly FUV/CR-irradiated molecular clouds expected in such intense starburst environments (Papadopoulos et al. 2011). Here we must note that the choice of the two representative α values is driven merely by the need to demonstrate the subthermal excitation of the

CI lines in a simple and straightforward manner (while bypassing the complexities and degeneracies of CO SLED-derived T_{kin} values). In practice even within galaxy regions, let alone entire galaxies with different SFR levels, the α factor will change as a function of $\langle n(\text{H}_2) \rangle$, $\langle U_{\text{CR}} \rangle$ (CR energy density), G_0 (FUV field strength) and $\langle M_s \rangle$ (average Mach number). If well-sampled molecular (e.g. CO, HCN, and their isotopologues), and atomic (CI) SLEDs and dust SEDs are available, the average α values can actually be extracted from the models (see Harrington et al. 2021 for a recent example). In turn, such α values can be used to determine the dominant power source of the ISM in the galaxy observed (i.e. the Y factor) with large α values indicative of volumetric (CR and/or turbulence) rather than FUV heating (see Papadopoulos et al. 2014 and references therein). We will briefly return to these issues at Section 3.

2.4 The non-LTE $R_{21/10}^{(\text{ci})} = F(n, T_{\text{kin}})$ ratio

The subthermal excitation of the CI lines must be partly the reason why they are often faint in galaxies, even as the CI 1-0 line has been successfully used as a global molecular gas tracer yielding gas masses in accordance with those deduced from the dust emission (and an assumed dust/gas ratio) and CO lines (e.g. Lee et al. 2021; Dunne et al. 2021). Under non-LTE conditions the CI 2-1 line luminosity will of course be much more sensitive to the average (n, T_{kin}) values in the ISM of galaxies than the CI 1-0 luminosity, which is what may be allowing the latter, even when faint, to remain a good molecular gas tracer (more details on this in Section 3).

The non-LTE CI line excitation in the ISM of galaxies readily deprives the $R_{21/10}^{(\text{ci})}$ ratio of its use as a molecular gas "thermometer" since now $R_{21/10}^{(\text{ci})} = F(n, T_{\text{kin}})$. The latter however makes the CI lines much more useful for studies of molecular gas conditions. Moreover unlike the optically thick CO rotational lines with their infinite-term partition function which necessitate: a) radiative transfer models with an upper J_{up} cutoff, b) assumptions about the line formation mechanism (LVG) and the corresponding expression for the line optical depth, and c) solving iteratively for level populations controlled by collisions *and* the local CO line radiation field itself, *the 3-level system of the two fine structure lines of the neutral atomic carbon can be solved analytically*. Thus the full non-LTE expression for $R_{21/10}^{(\text{ci})} = F(n, T_{\text{kin}})$ can be obtained without assumptions about gas velocity fields and their impact on line formation and optical depth.

The latter is possible only for optically thin CI lines, which early observations of dense molecular clouds showed it to be the case (Zmuidzinas et al. 1988), as well as in the bulk of the ISM in galaxies (Weiss et al 2003 and references therein; Harrington et al. 2021). Low line optical depths is among the traits that allow the CI 1-0 line to trace molecular gas mass (CI-based H₂ mass estimates are always made under the optically thin line assumption), on par with other optically thin tracers such dust and ¹³CO line emission. Regarding the latter, the good spatial and intensity correlation between CI 1-0 and ¹³CO J=2-1 line emission in molecular clouds (an important early landmark in the case against a PDR-only origin of CI line emission, Keene et al. 1997) would be difficult to achieve unless both lines were mostly optically thin⁶.

The non-LTE expressions for the CI 3-level populations as

⁴ Moreover lower density gas is also warmer gas (since dominant cooling has $\Lambda \propto n^2$) further enhancing the contribution of the lower density gas to the CI line luminosities.

⁵ when imaged to be studied individually these CR-dominated regions are very important as the sites where the initial conditions of star formation are set (Bergin & Tafalla 2007).

⁶ Should any cases of optically thick CI lines over large molecular gas mass reservoirs be found in galaxies, detailed line radiative transfer in macro-turbulent media must then be employed. CI line emission models, while

functions of density, temperature and background radiation field are used to compute the $R_{21/10}^{(ci)} = F(n, T_{kin})$ function (see Papadopoulos, Thi & Viti 2004, Appendix), and then plot it in Figure 4. There we overlay the measured $R_{21/10}^{(ci)}$ values, to which we assign the corresponding $T_{kin} = \alpha T_{dust}$ for the concomitant molecular gas, using the T_{dust} obtained for the particular object, and a gas-dust thermal decoupling factor α (see 2.3.1). Here it is worth pointing out that the value $\alpha=1.2$ adopted for the entire sample (Figure 4, left panel) is almost certainly too low for the ISM of starburst galaxies whose actual average T_k will be higher. In that regard the characteristic density of the iso-density curve crossing through a particular $[(R_{21/10}^{(ci)})_{meas}, T_{kin}]$ point in our $R_{21/10}^{(ci)} = F(n, T_{kin})$ diagram (Figure 4) is an upper limit to the average density of the molecular gas. In the right panel where a higher value $\alpha=2.5$ was adopted for the starburst galaxies in the sample, the corresponding points move to the lower- n /higher- T_k non-LTE part of the diagram.

Figure 4 shows again that, for $n \sim n_{ik,crit} = A_{ik} / (\sum_k C_{ik})$ (sum of collisional coefficients "running" for both $k < i$ and $k > i$ values of k) the corresponding $i \rightarrow k$ transition does not become thermalized (where $T_{ex}(i, k) \sim T_k$). Indeed for $n \sim n_{2-1,crit} \sim 10^3 \text{ cm}^{-3}$ the CI 2-1 line remains very subthermally excited, yielding $R_{21/10}^{(ci)} \sim 1-1.8$ (LTE values for $T_{kin} = 30-100 \text{ K}$: $\sim 1.5-3.8$), and only for $n \sim (1-3) \times 10^4 \text{ cm}^{-3}$ the line ratio starts approaching its LTE values.

Finally Figure 4 indicates the reason behind the curious clustering of the (CI line/LTE)-derived gas temperatures within a narrow range of $\sim 20-30 \text{ K}$ which was attributed to weakly varying average molecular gas temperatures across galaxy populations (Valentino et al. 2020). It is instead simply an effect of subthermal CI 2-1 line excitation (and a population "pile" up on the $J=1$ level, $E_1/k_B \sim 24 \text{ K}$), under the typical densities of the molecular gas in the ISM of galaxies not weakly varying gas temperatures. Should all the observed CI line ratios be interpreted using solely the LTE curve (yellow), the deduced T_k (CI, LTE) would be contained within the $\sim 20-30 \text{ K}$ range, while for numerous Main Sequence galaxies such LTE-based interpretation would suggest average gas temperatures as low as $\sim 15 \text{ K}$, typical for the ISM of SF-quiescent not of SF-active galaxies. On the other hand, for non-LTE excitation and e.g. $n = 10^3 \text{ cm}^{-3}$, the CI line ratio stays within a narrow range of values ($\sim 1-1.8$) even as $T_k = (30-100) \text{ K}$ (a more representative range for the ISM of galaxies with a wide range of SFRs). Should the corresponding CI line ratios be interpreted in the LTE regime, it would yield T_k (CI, LTE) $\sim 30 \text{ K}$ for the SF-extreme group.

3 DISCUSSION

The subthermal excitation of the CI lines has been predicted theoretically by Glover et al. 2015 using turbulent cloud simulations, which also found the CI 1-0 line emission to be a good H_2 cloud structure and mass tracer, albeit for rather small clouds ($10^4 M_\odot$) rather than the typical Giant Molecular Clouds in galaxies ($\sim 10^5-10^6 M_\odot$). Our study lends strong observational support to this view, which will impact molecular gas mass estimates based on the CI lines, via the so-called $Q_{10} = N_1/N_{tot}$ and $Q_{21} = N_2/N_{tot}$ factors which now become dependant on both the average density and temperature of the molecular gas. In Figure 5 we show the $Q_{10,21}(n, T_k)$ functions obtained from available analytic expressions. As expected the

no longer analytical, would nevertheless still be simpler than those for the infinite J -ladder of CO lines.

largest sensitivity is shown by $Q_{21}(n, T_k)$ which varies as $\sim 0.05-0.45$ for $T_{kin} = (20-100) \text{ K}$ and $n = (10^2-10^5) \text{ cm}^{-3}$, where it remains $T_{ex}(2, 1) \lesssim T_{kin}$ (i.e. $Q_{21} \lesssim Q_{21}(\text{LTE})$).

There is markedly less variation of the Q_{10} factor which, for the same (n, T_k) range, is: $\sim 0.3-0.5$. Perhaps surprisingly, for $n \geq 10^3 \text{ cm}^{-3}$, its non-LTE values slightly exceed the LTE ones (i.e. $T_{ex}(1, 0) \gtrsim T_{kin} \Leftrightarrow Q_{10} \gtrsim Q_{10}(\text{LTE})$) when $T_k \gtrsim 30 \text{ K}$. Such slight superthermal excitation occurs because of a "pile" up on the $J=1$ level induced by a faster $J=2 \rightarrow 1$ than $J=1 \rightarrow 0$ spontaneous de-excitation (for the CI lines: $A_{21}/A_{10} \sim 3.38$) once temperatures are high enough for collisions to start populating the $J=2$ level (radiative and collisional de-excitation of $J=2 \rightarrow 0$ is negligible). A similar effect can occur for the CO $J=2-1$ and $J=1-0$ transitions as noticed first by Goldsmith 1972 and described in more detail by Leung & Liszt 1976 (see also de Jong et al. 1975), though mostly for the ^{13}CO isotopologue as the high optical depths of the CO lines act to suppress such non-LTE effects.

The stronger variation of the Q factors in the non-LTE regime will affect the CI-based molecular gas mass estimates, adding one more source of uncertainty (besides that of the $X_{CI} = [C/H_2]$ abundance) to the molecular gas mass/line luminosity ratio $M(H_2)/L_{CI} \propto (X_{CI} Q_{ik})^{-1}$. From Figure 5 the mean value of Q_{10} for most of the expected average ISM conditions: $[n, T_{kin}] = [(300 - 10^4) \text{ cm}^{-3}, (25 - 80) \text{ K}]$ is $\langle Q_{10} \rangle = 0.48$ with $\lesssim 16\%$ variation (99th percentiles), and adopting it is adequate for molecular gas mass estimates via the CI 1-0 line for most average ISM conditions.

For the CI 2-1 line on the other hand, care must be taken to determine the appropriate Q_{21} factor if this line (when detected) is to be used to estimate the underlying molecular gas mass. This can be performed statistically per galaxy population, in conjunction with other molecular gas mass tracers (dust, CO, ^{13}CO) (Dunne 2019; Dunne et al. 2021). Alternatively, joint CI, CO SLED and dust SED models are a powerful way to constrain the average ISM thermal, dynamical and even chemical states of the ISM in individual galaxies, with total H_2 gas mass estimates a mere byproduct (e.g. Papadopoulos et al. 2014; Harrington et al. 2021). Future modeling efforts should incorporate the analytical 3-level CI line emission model, *without any assumptions about the underlying velocity field (and its role on the line formation mechanism)*. This is bound to yield more robust models that are less sensitive to the well-known n - T_k CO SLED model degeneracies. The latter are due to the significant CO line optical depths, and the common expression used to incorporate the Large Velocity Gradient (LVG) assumption into the formula for the line escape probability $\beta_{ik} = f(n, T_k, dV/dR)$ for CO line emission (which is unnecessary for the CI lines).

The aforementioned promise of an analytical model of the 3-level CI line emission incorporated in joint molecular SLED and dust emission SED fits cannot be fully realized without including some new astrochemistry, the one regulating the average $R_C = [C/H_2]$ abundance in the ISM (entering the expressions for all relative C and CO line strengths). It is expected that $R_C = f(n, \langle U_{CR} \rangle, Z)$, with astrochemical modelling now mature enough to provide such functions, even if empirical ones (see Bisbas et al. 2015 for such a function for the CO/ H_2 abundance). With adequate line and continuum data, such astrochemically-informed joint CO/CI SLED and dust emission SED fits hold the additional promise of tying an important extragalactic parameter, the average SFR density of galaxies $\rho_{SFR} \propto \langle U_{CR} \rangle$, to ISM line and continuum observables. The latter may not sound much of a feat until one realizes: a) the difficulty of practically constraining a quantity like ρ_{SFR} , especially in deeply dust-enshrouded mergers and the clumpy SF disks typical at high

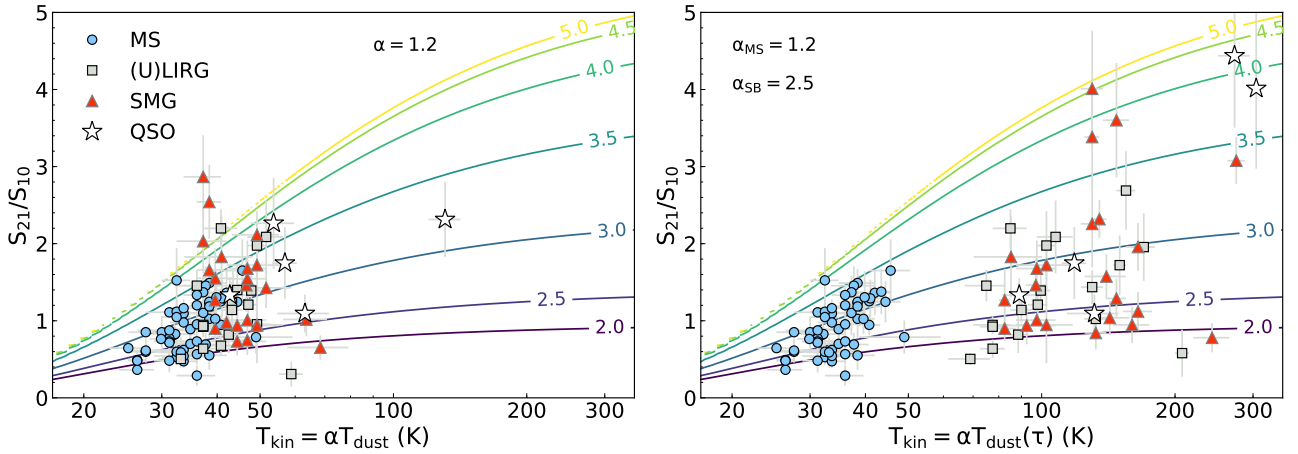


Figure 4. The $R_{21/10}^{(ci)}$ ratio versus T_k for a range of gas densities (shown as iso-density lines labelled by the corresponding $\log(n)$ values). The data from our sample are over-plotted using the same symbols as Figure 2: blue circles (Main Sequence galaxies), red triangles (high- z SMG), stars (QSO) and grey squares (local (U)LIRGS). **Left panel:** We used the luminosity-weighted T_d to derive T_k using constant gas-dust thermal decoupling factor $\alpha=1.2$ (Section 2.3.1). **Right panel:** Using the optically thick dust SED fit results where appropriate to derive T_d (and hence $T_k = \alpha T_d$) and to correct the measured $R_{21/10}^{(ci)}$ for the effects of the dust optical depth, see Section 2.1). In this panel we use a higher value of $\alpha=2.5$ for the extreme star-bursts as deduced by Harrington et al. (2021) for such galaxies.

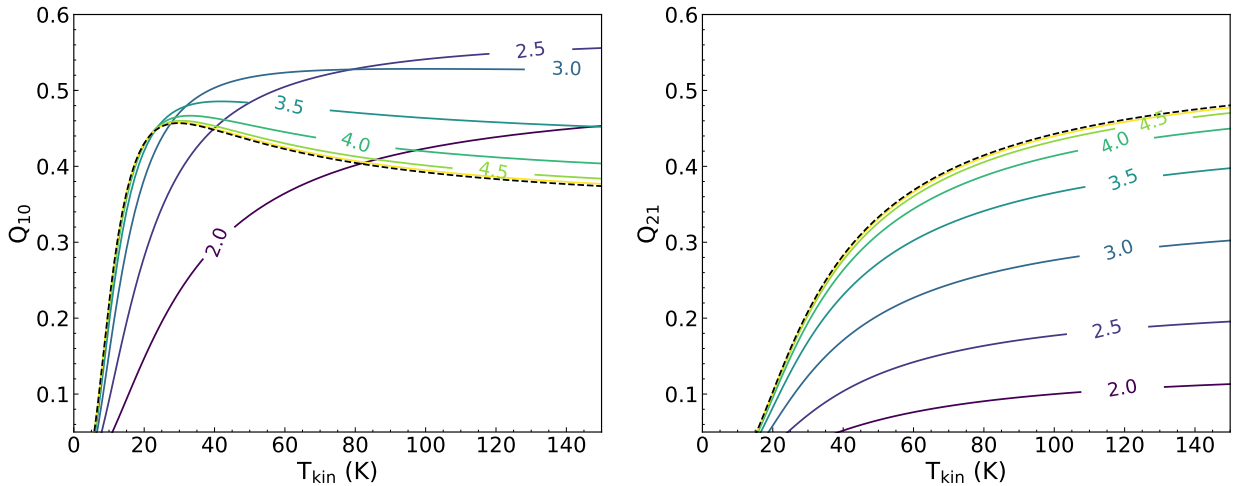


Figure 5. The $Q_{10}(n, T_k)$ (left) and the $Q_{21}(n, T_k)$ (right) factors, for a range of gas densities and temperatures expected for the ISM of galaxies. Iso-density curves are labelled with $\log(n) / \text{cm}^{-3}$, the LTE curve is shown as a black dashed line. It is note-worthy that for $Q_{10}(n, T_k)$, the lower density curves lie above the LTE values for $T_k > 20\text{--}30$ K (suprathermal) a behaviour explained in section 3. Thus using the $Q_{10}(\text{LTE})$ value at $T_k \sim 30$ K will produce a *slight systematic overestimate* of the C_I mass (and hence H₂ mass) when using CI(1–0) as a H₂ tracer. For higher T_k this effect becomes more pronounced but is still $< 35\%$. Thus it does not pose a serious problem in the use of the CI(1–0) as a H₂ tracer (unlike the adopted value of the CR-controlled $[\text{C}/\text{H}_2]$ abundance). For the CI(2–1) line, the calibration as a tracer of H₂ is far less straight-forward due to the large variation in Q_{21} (0.05–0.45) at a given T_k , once we accept that the system is in non-LTE, while in the ISM of some galaxies this line can be very faint because its low sub-thermal excitation.

redshifts, and b) the role of ρ_{SFR} in setting the SF initial conditions in the ISM of galaxies, and perhaps also the stellar IMF (Papadopoulos et al. 2011).

3.1 Molecular gas reservoirs outside SF galaxies: the CI line ratio versus T_{dust} as an indicator?

A few of the most extreme starbursts in our sample ($\text{SFR} \gtrsim 500 M_{\odot} \text{yr}^{-1}$) have such low global CI line ratios ($\lesssim 1$), that can only be accommodated by very low gas densities $n \sim (10^2 - 3 \times 10^2) \text{cm}^{-3}$ (Figure 4, right panel). This is because their high

T_{kin} values (deduced from the high T_{dust} of their global SEDs), place them to the low- n /high- T part of Figure 4. Such densities are near to the lowest ones found in Galactic GMCs, and ‘hover’ near the $\text{HI} \rightarrow \text{H}_2$ phase transition limit expected for Galactic FUV fields ($G_0 \sim 1$) in metal-rich ISM ($Z=1$). The latter sets an absolute lower limit for gas densities if H₂ is to form appreciably in a given FUV radiation and metallicity environment (e.g. Papadopoulos, Thi & Viti 2002), a limit that can only be higher in the much more FUV-intense ISM environments of extreme starbursts. Finally it is unexpected to have such very low density gas dominate the global CI line emission of some of the most extreme starbursts, where large mass fractions of high density ($\sim 10^4 \text{cm}^{-3}$) molecular gas are expected (Gao &

Solomon 2004). We speculate that the low-density gas component implied by the low global CI line ratios in some of the most extreme starbursts of our sample does not reside inside those galaxies, but outside, associated with powerful molecular gas winds, and/or massive reservoirs of Circumgalactic (CG) gas and dust. Such reservoirs have been found around starbursts and AGN (Cicone et al. 2018, 2021) results of powerful SF and/or AGN feedback on the ISM of galaxies. Global CI line emission in such objects may thus have substantial contributions from such CG and/or wind-related H₂ gas down to very low densities⁷.

In summary the observed very low CI(2-1)/(1-0) ratios and high T_{dust} values are used (under the 1-component assumption for CI line and dust continuum emission) to deduce H₂ gas densities that are far too low to belong to typical GMC structures. Moreover this is obtained for some of the most extreme starbursts in the sample whose highly turbulent ISM, if anything, is expected to have most of the H₂ mass of the resident GMCs in the high density domain (> 10³ cm⁻³). We thus consider it more likely that the implied low density H₂ gas belongs to a massive molecular wind and/or CG gas and dust component outside these starbursts.

Of course in practice our global CI ratios and dust SEDs encompass *both* the starburst ISM and the wind/CG H₂ gas and dust reservoir, each with its own distinct average $\alpha > 1$ values, the modest ones associated with the starburst ISM, and the higher ones with the wind and/or CG H₂ gas and dust reservoirs outside the galaxies. In the latter case the dust (far from the SF-powered FUV-fields inside the starburst) will be cold, while the H₂ gas will continue to be heated by starburst-produced CRs (that readily convect out with the molecular winds) and by shocks, yielding α values higher than those in the starburst ISM. In this simple 2-component variation of the 1-component framework used in this study, the 1-component "composite" α will be skewed towards the high $\langle\alpha\rangle=2.5$ values found by Harrington et al. 2021, because of a massive wind/CG H₂ and dust component present outside their extreme starbursts. However the relative gas mass ratios between these two components cannot be confidently constrained using global SLEDs and dust SEDs like the ones used here, but only with spatially resolved CI and low-J CO line imaging observations *that remain sensitive to large scale molecular gas distributions*⁸

Finally the global CI line ratios (along with well-sampled global dust SEDs for constraining $\langle T_{\text{dust}} \rangle$) may be good indicators of galaxies with possible massive, low-density, reservoirs of CG and/or molecular gas winds for reasons that go beyond their excitation sensitivity to the presence of very low density H₂ gas that is thermally decoupled from its concomitant dust. It is because in the CR-irradiation environments of CG and molecular wind material very low-density gas $\sim(50-200)\text{ cm}^{-3}$ will be very CO poor (Papadopoulos et al. 2018) and thus very faint even in low-J CO line emission. Moreover, even if CO could somehow form efficiently at such low densities while being subjected to the CR energy densities of the wind/CG environments, the high-J CO lines necessary for probing high-T_{kin} gas (and thus for identifying molecular gas and dust with extreme gas-dust thermal decoupling) unfortunately also have considerable critical densities. Indicatively CO 4-3, with $E_4/k_B \sim 55\text{ K}$ (comparable to the $E_2/k_B \sim 62\text{ K}$ of the CI 2-1 line, has $n_{\text{crit}} \sim 2 \times 10^4\text{ cm}^{-3} \sim 20 \times n_{\text{crit}}(\text{CI}, 2-1)$. Such high-J CO lines

will thus be faint for warm *and* low density gas in molecular gas winds and CG reservoirs, and imaging their emission cannot reveal their true extent and mass around galaxies. Their global (unresolved) emission on the other hand will be dominated by the starburst ISM rather than by the feebly emitting (in high-J CO lines) molecular wind and CG gas reservoirs.

Of course, once a candidate starburst/AGN is selected for the possible presence of massive H₂ wind and/or CG reservoirs using the global CI line/dust emission criterion, deep CO line imaging of low-J CO lines⁹ remains valuable for independently identifying the CO-rich parts of the wind and/or CG molecular gas reservoirs, and outlining their distribution and kinematics (see Cicone et al. 2021 for a recent such result). Sensitive CI line interferometric imaging, that includes short spacing and total power measurements (so that extended emission from the CG and/or molecular gas wind reservoir is not resolved out), can then uncover any CO-poor low density H₂ gas along with the CO-rich one.

In the case of the high frequency CI lines such observations can be challenging, carrying the very real possibility of resolving out much of the extended CG and molecular gas wind emission. This necessitates the most compact ALMA/ACA configurations aided by deep observations in total power (TP) mode. In that regard, the planned 50-m class AtLAST submm telescope in the Atacama Desert¹⁰, with a combination of suitable heterodyne receivers and bolometers, can be a search "machine" for massive, thermally-decoupled, molecular gas and dust reservoirs around distant SF galaxies and QSOs, outcomes of strong AGN and/or SF feedback processes across the Universe. When it comes to imaging such reservoirs around the candidate objects, spectral lines of low-J CO and CI (for H₂), and CII (for H₂, HI, and HII), may be the sole capable tracers since the dust continuum may be very faint because of the low dust temperatures expected far from the starburst/AGN¹¹, and the expected high gas-dust thermal decoupling at low gas densities.

4 CONCLUSIONS

Guided by an ever increasing body of CI 1-0, 2-1 line luminosity data for galaxies across cosmic epoch, and their use as alternative molecular gas temperature and mass distribution tracers, we assembled a large dataset of 106 galaxies with available total CI 2-1 and 1-0 line luminosities in order to examine their excitation levels over galaxy-sized molecular gas mass scales. Using the analytical solutions of the 3-level system responsible for the CI lines, the dust temperatures obtained from global dust emission SEDs available for our sample, along with the expected gas-dust thermal decoupling factors for FUV/CR-irradiated ISM, we reached the following conclusions:

- The CI lines are subthermally (non-LTE) excited over the bulk of the ISM of galaxies, and as such their ratio cannot be used as a probe of average molecular gas temperatures.

⁹ J=1-0, 2-1, 3-2, so that their (radiative-trapping)-reduced critical densities remain $\lesssim 10^3\text{ cm}^{-3}$ and do not become overly biased against low-density gas.

¹⁰ <https://www.atlast.uio.no/>

¹¹ At high redshifts the difficulty of imaging such reservoirs, no matter how massive, via their dust continuum, is further compounded by their immersion in a rising CMB, inducing very low dust-CMB emission contrast (Zhang et al. 2016)

⁷ Sensitive CI 1-0 ALMA imaging has already revealed a massive outflow H₂ gas reservoir around the local starburst NGC 6240 (Cicone et al. 2018)

⁸ Dust emission may not be a good bet for the CG/wind component as the dust outside galaxies is expected to be very cold (< 15 K).

- The recently reported small variation of the average molecular gas temperatures in galaxies, deduced using the CI line ratio and the assumption of LTE, is an artifact of the non-LTE CI line excitation conditions, and does not reflect actual average molecular gas temperatures.

- The non-LTE line excitation impacts the molecular gas mass estimates based on the CI lines. For the CI 1-0 line, adopting the mean non-LTE excitation factor $\langle Q_{10} \rangle = 0.48$ is adequate, as it varies little ($\sim 16\%$) over typical ISM conditions variations. For the CI 2-1 line this uncertainty is much larger with the corresponding Q_{21} factor varying over $\sim 0.05\text{--}0.45$.

- The analytical non-LTE expression of the CI 2-1/1-0 line ratio $R_{21/10}^{(ci)}(n, T_k)$ can be used in joint models with CO lines and dust emission SEDs without adopting the assumptions used for CO line radiative transfer models (i.e. Large Velocity Gradient velocity fields and local escape probability expressions depending on them and the assumed cloud geometry). This will add robustness in future joint CI/CO SLED and dust SED models for the ISM of galaxies.

- Some of the lowest ($\lesssim 1$) global CI(2-1)/(1-0) line ratios and high average T_{dust} values (and thus T_{kin}) are found in some of the most extreme starbursts of our sample, indicating large amounts of warm but very low density molecular. We conjecture that this molecular gas reservoir is outside the starburst/AGN, part of a powerful wind and/or Circumgalactic (CG) material, and propose this combination of low CI(2-1)/(1-0) and high T_{dust} values as a criterion to locate them.

DATA AVAILABILITY

No new data were generated or analysed in support of this research.

ACKNOWLEDGEMENTS

We would like to thank the anonymous referee for comments that allowed us to clarify issues regarding CI line optical depths, as well the astrophysics behind the gas-dust thermal decoupling and the possible values of the α parameter in galaxies. The latter directly informed our now expanded discussion in section 3.1.

Finally we thank our few remaining friends for keeping us old sailors onboard the pirate ship of Discovery, and not tossing us overboard, to the placid Sargasso Seas of irrelevance and Oblivion. PPP would like to thank Seren for being such an accommodating little angel during his visit in Cardiff when he experimented endlessly in the kitchen, and her parents survived...

REFERENCES

- Aalto, S. Booth, R. S., Black, J. H., Johansson, L. E. B. 1995, *A&A*, 300, 369
- Alaghband-Zadeh, S., Chapman, S. C., Swinbank, A. M. et al. 2013, *MNRAS*, 435, 1493
- Andreani, P., Retana-Montenegro, E., Zhang, Z.-Y. et al. 2018, *A&A*, 615, 142
- Aniano, G., Draine, B. T., Hunt, L. K. et al. 2020, *ApJ*, 889, 150
- Banerji, M., Jones, G. C., Wagg, J. et al. 2018, *MNRAS*, 479, 1154
- Bergin, E. A., & Tafalla, M. 2007, *Annual Review of Astronomy & Astrophysics*, vol. 45, Issue 1, pg 339
- Bothwell, M. S., Aguirre, J. E., Aravena, M., et al. 2017, *MNRAS*, 466, 2825
- Boogaard, L. A., van der Werf, P. Weiss, A. et al. 2020, *ApJ*, 902, 109
- Bisbas, T. G., Papadopoulos, P. P., & Viti, S. 2015, *ApJ*, 803, 37
- Bisbas, T. G., van Dishoeck, E. F., Papadopoulos, P. P., et al. 2017, *ApJ*, 839, 90
- Boettcher, E. et al. 2020, *A&A*, 637, 17
- Canámeras, R., Yang, C., Nesvadba, N. P. H. 2018, *A&A*, 620, 61
- Chang, Z., Zhou, J., Wilson, C. D. et al. 2020, *ApJ*, 900, 53
- Chu, J. K., Sanders, D. B., Larson, K. L. et al. 2017, *ApJS*, 229, 25
- Cicone, C., Severgnini, P., Papadopoulos, P. P. et al. 2018, *ApJ*, 863, 143
- Cortzen, I., Magdis, G. E., Valentino, F. et al. 2020, *A&A*, 634, L14
- Crocker, A. F., Pellegrini, E., Smith, J.-D. T. et al. 2019, *ApJ*, 887, 105
- Clark, P. C., Glover, S. C. O., Ragan, S. E., & Duarte-Cabral, A. 2019, *MNRAS*, 486, 4622
- Clark, C. J. R., Verstocken, S., Bianchi, S. et al. 2018, *A&A*, 609, 37
- Dunne, L., Maddox, S. J., Vlahakis, C., & Gomez, H. L. 2021, *MNRAS*, 501, 2573
- Emonts, B. H. C., Lehnert, M. D., Dannerbauer, H. et al. 2018, *MNRAS*, 477, L60
- Falstad, N. et al. 2021, *A&A*, 649, 105
- Gao Y. & Solomon P. M. 2004, *ApJS*, 152, 63
- Garcia-Gonzalez, J., Alonso-Herrero, A., Hernan-Caballero, A. et al. 2016, *MNRAS*, 458, 4512
- Glover, S. C. O., Clark, P. C., Micic, M., & Molina, F. 2015, *MNRAS*, 448, 1607
- Glover, S. C. O., & Clark, P. C. 2016, *MNRAS*, 456, 3596
- González-Alfonso, E & Sakamoto, K, 2019, *ApJ*, 882, 153
- Hao, C.-N., Kennicutt, R. C., Johnson, B. D. et al. 2011, *ApJ*, 741, 124
- Harrington, K. C., Weiss, A., Yun, M. S. et al. 2021, *ApJ*, 908, 95
- Hollenbach, D. J., Takahashi, T., & Tielens, A. G. G. M. 1991, *ApJ*, 377, 192
- Hollenbach, D. J., & Tielens, A. G. G. M. 1999, *Reviews of Modern Physics*, Volume 71, Issue 1, pp.173-230
- Israel, F. P., Tilanus, R. P. J., & Baas, F. 1998, *A&A*, 339, 398
- Israel, F. P., Rosenberg, M. J. F., van der Werf, P. P. et al. 2015, *A&A*, 578, 95
- Ikeda, M., Oka, T., Tatematsu, K., et al. 2002, *ApJS*, 139, 467
- Izumi, T., Nguyen, D.-D., Imanishi, M. et al. 2020, *ApJ*, 898, 75
- Jiao, Q., Zhao, Y., Zhu, M. et al. 2017, *Astrophys. Lett.*, 840, L18
- Jiao, Q., Zhao, Y., Lu, N. et al. 2019, *ApJ*, 880, 133
- Jiao, Q., Gao, Y., & Zhao, Y. 2021, *MNRAS*, 504, 2360
- Kamenezky, J., Rangwala, N., Glenn, J. et al. 2014, *ApJ*, 795, 174
- Keene, J., Blake, G. A., Phillips, T. G., et al. 1985, *ApJ*, 299, 967
- Keene, J., Blake, G. A., & Phillips, T. G. 1986, *Bulletin of the American Astronomical Society*, Vol. 18, pg 637
- Keene, J., Lis D. C., Phillips, T. G., & Schilke, P. 1997, *IAU Symposium*, No. 178 (Molecules in Astrophysics) p. 129 - 139, (Eds E. F. van Dishoeck)
- Kennicutt, R. C. & Evans, N. J. 2012, *ARA&A*, 50, 531
- Lapham, R. C. & Young, L. M. 2019, *ApJ*, 875, 3
- Lelli, F., De Breuck, C., Falkendal, T. 2018, *MNRAS*, 479, 5440
- Lu, N., Zhao, Y., Diaz-Santos, T. et al. 2017, *ApJS*, 230, 1
- Lu, N., Cao, T., Diaz-Santos, T. et al. 2018, *ApJ*, 864, 38
- Man, A. W. S., Lehnert, M. D., Vernet, J. D. R. et al. 2019, *A&A*, 624, 81
- Michiyama, T., Ueda, J., Tadaki, K. et al. 2020, *Astrophys. Lett.* 897, L19
- Miyamoto, Y., Seta, M., Nakai, N. et al. 2018, *PASJ*, 70, L1
- Miyamoto, Y., Yasuda, A., Watanabe, Y. et al. 2021, *PASJ*, 34
- Murphy, E. J., Condon, J. J., Schinnerer, E. et al. 2011, *ApJ*, 737, 67
- Nesvadba, N. P. H., Canámeras, R., Kneissl, R. et al. 2019, *A&A*, 624, 23
- Offner, S. S. R., Bisbas, T. G., Bell, T. A., & Viti, S. 2104, *MNRAS*, 440, 810
- Ojha, R., Stark, A. A., Hsieh, H. H., et al. 2001, *ApJ*, 548, 253
- Oka, T., Yamamoto, S., Iwata, M., et al. 2001, *ApJ*, 558, 176
- Papadopoulos, P. P., Thi, W.-F., Viti, S. 2002, *ApJ*, 579, 270
- Papadopoulos, P. P., Thi, W.-F., & Viti, S. 2004, *MNRAS*, 351, 147
- Papadopoulos, P. P., van der Werf, P., Isaak, K., & Xilouris, E. M. 2010a, *ApJ*, 715, 775

- Papadopoulos, P. P., Isaak, K., van der Werf, P. 2010b, *ApJ*, 711, 757
- Papadopoulos, P. P., Thi, W.-F., Miniati, F., & Viti, S. 2011, *MNRAS*, 414, 1705
- Papadopoulos, P. P., Zhang, Z.-Y., Xilouris, E. M. et al. 2014, *ApJ*, 788, 153
- Papadopoulos, P. P., Bisbas, T., & Zhang, Z.-Y., 2018, *MNRAS*, 478, 1716
- Pereira-Santaella, M., Spinoglio, L., Busquet, G. et al. 2013, *ApJ*, 768, 55
- Plume, R., Jaffe, D. T., & Keene, J. 1994, *Astrophys. Lett.*, 425, L49
- Popping, G., Decarli, R., Man, A. W. S. 2017, *A&A*, 602, 11
- Pineda, J. L., & Bensch, F. 2007, *A&A*, 470, 615
- Rosenberg, M. J. F., van der Werf, P. P., Aalto, S. et al. 2015, *ApJ*, 801, 72
- Salak, D., Nakai, N., Seta, M., Miyamoto, Y. 2019, *ApJ*, 887, 143
- Saito, T., Michiyama, T., Liu, D. et al. 2020, *MNRAS*, 497, 3591
- Schumacher, H., Martinez-Sansigre, A., Lacy, M. et al. 2012, *MNRAS*, 423, 2132
- Schirm, M. R. P., Wilson, C. D., Parkin, T. J. et al. 2014, *ApJ*, 781, 101
- Scoville, N. et al. 2015, *ApJ*, 800, 70
- Spaans, M. & van Dishoeck E. F. 1997, *A&A*, 323, 953
- Stacey, G. J., Aravena, M., Basu, K. et al. 2018, *Proceedings of the SPIE*, Volume 10700, pp. (2018)
- Stutzki, J., Bensch, F., Heithausen, A. et al. 1998, *A&A*, 336, 697
- Tanaka, K., Oka, T., Matsumura, S., et al. 2011, *Astrophys. Lett.*, 743, L39
- Tatematsu, K., Jaffe, D. T., Plume, R. et al. 1999, *ApJ*, 526, 295
- Valentino, F., Magdis, G. E., Daddi, E. et al. 2020, *ApJ*, 890, 24
- Valentino, F., Magdis, G. E., Daddi, E. et al. 2018, *ApJ*, 869, 27
- Wall, W. F., Jaffe, D. T., Bash, F. N., Israel, F. P., Maloney, P. R., & Baas, F. 1993, *ApJ*, 414, 98
- Walter, F., Weiss, A., Downes, D. et al. 2011, *ApJ*, 730, 18
- Weiss, A., Henkel, C., Downes, D., & Walter, F. 2003, *A&A*, 409, L41
- Weiss, A., Downes, D., Neri, R. et al. 2007, *A&A*, 467, 955
- Yamagishi, M., Shimajiri, Y., Tokuda, K. et al. 2021, *Astrophys. Lett.*(in press) (arXiv 210406030Y)
- Zmuidzinas, J., Betz, A. L., Boreiko, R. T., & Goldhaber, D. M. 1988, *ApJ*, 335, 774
- Zhang, Z.-Y., Papadopoulos P., Ivison R. J., Galametz M., Smith W. K., & Xilouris E. M. 2016 *Royal Society Open Science*, Vol.3, Issue 6

This paper has been typeset from a $\text{\TeX}/\text{\LaTeX}$ file prepared by the author.